Preparation and electronic properties of $Sr_{2-x}La_xRhO_4$

Tetsuo Shimura, Mitsuru Itoh, Yoshiyuki Inaguma, and Tetsurō Nakamura
Research Laboratory of Engineering Materials, Tokyo Institute of Technology, 4259 Nagatsuta-cho, Midori-ku, Yokohama 227, Japan
(Received 28 June 1993)

K_2NiF_4-type solid solution system $Sr_{2-x}La_xRhO_4$ was prepared and the structure and electrical and magnetic properties were investigated. The result of powder x-ray-diffraction analysis shows stretching of the a and b axes and shortening of the c axis with an increase of x. The positive temperature dependence of the resistivity in the range $x \leq 0.15$ disappears with an increase of x greater than 0.15. The temperature dependence of the activation energy of carriers suggests two-dimensional variable range hopping-type conduction in the semiconducting range. The localized magnetic moment of the Rh ion is greater than the calculated value based on the low spin state, and the antiferromagnetic interaction among Rh ions decreases with an increase of x. A magnetic anomaly around 60 K observed for Sr_2RhO_4 diminishes with an increase of x and vanishes at $x=0.20$. A positive Seebeck coefficient suggests hole conduction in this system and the Fermi energy obtained from the linear temperature dependence of the Seebeck coefficient on T decreases with x, which can be explained from the decrease of holes with the substitution of low spin $Rh^{3+}(4d^6)$ for $Rh^{4+}(4d^5)$.

INTRODUCTION

Since the discovery of high-temperature superconductivity, much attention has been paid to the electrical and magnetical properties of a K_2NiF_4-type complex oxide. The formula of this type of oxide is expressed as A_2BO_4, and this structure is well described as the alternate stacking of one rock-salt slab AO and one perovskite slab ABO_3. Ganguri[1] pointed out that a K_2NiF_4 structure is stabilized when the ratio r_A/r_B takes a value between 1.7 and 2.4, and where r_A and r_B are the ionic radii of A and B, respectively. Poix[2] reported that the tolerance factor t given by $(r_A+r_B)/\sqrt{2}(r_B+r_O)$, where r_O is the ionic radius of the oxygen ions, needs to take a value between 0.85 and 1.02 for stabilization of this structure.

The properties of a K_2NiF_4-type complex oxide depend mainly on the electron configuration of the B ion. In the case of the B ion having partly filled $4d$ orbitals, the anticipated electronic configuration of $4d$ electrons is a low spin state, because the expanse of the $4d$ orbital is so much greater than that of the $3d$ orbital that the repulsion force acting between the two electrons in the same $4d$ orbital becomes smaller than that in the $3d$ orbital. Rh^{4+} and Rh^{3+} have five and six $4d$ electrons, respectively. The configuration of $4d$ electrons in low-spin Rh^{4+} and Rh^{3+} are $4d\varepsilon^5 4d\gamma^0$ and $4d\varepsilon^6 4d\gamma^0$, respectively. This means that low-spin Rh^{4+} has one hole in the $4d\varepsilon$ orbital if the anticipation is true. It is interesting to investigate the properties of the complex oxide with a K_2NiF_4 structure which has Rh^{4+} or Rh^{3+} at the B site.

Randhaul and Wold[3] reported the existence of Sr_2RhO_4 at a temperature region between 1200 and 1300 °C, and also reported its lattice parameter of a body-centered tetragonal unit cell with $a=0.3850$ nm and $c=1.290$ nm. We successfully achieved single-phased Sr_2RhO_4, and measured the temperature dependence of electric resistivity and magnetic susceptibility down to 10 or 5 K.[4] $SrLaRhO_4$ was first prepared by Blasse,[5] and was reported to have a tetragonal lattice parameter with $a=0.392$ nm and $c=1.278$ nm.

In this paper, we report on the preparation of a solid solution between Sr_2RhO_4 and $SrLaRhO_4$. The low-spin state of Rh^{3+} in the perovskite-type structure $LaRhO_3$ has already been confirmed by the present authors.[6] Electronic configurations in Rh^{3+} and Rh^{4+} ions in $Sr_{2-x}La_xRhO_4$ are expected to be low-spin states.

In this study, structural analysis by powder x-ray-diffraction analysis and measurement of resistivity, magnetic susceptibility, and Seebeck coefficients was carried out for $Sr_{2-x}La_xRhO_4$.

PREPARATION AND EXPERIMENT

All samples were prepared by the conventional solid-state reaction method. The starting materials were $SrCO_3$ (99.9%), La_2O_3 (99.9%), and Rh_2O_3 (99.9%) in a high-temperature form.[7] A stoichiometric amount of these powders was mixed in an agate mortar with ethanol. The total weight of the mixture was about 600–700 mg. The dried mixture was pressed into a pellet 1 mm in thickness and 12 mm in diameter, under a static pressure of about 80 MPa. The pellet was calcinated at 1473 K for 12 h in an O_2 gas flow. Then the pellet was cooled to room temperature and reground in an agate mortar, followed by mixing and pelletization. This pellet was sintered at 1523 K for 36 h in an O_2 gas flow.

Phase characterization and determination of the lattice symmetry, space group, and lattice parameter were carried out using x-ray-diffraction analysis. The diffraction data were collected using a Rigaku θ-θ diffractometer with monochromator. Cu $K\alpha$ radiation ($\lambda=0.15405$ nm) was used for the experiment. The electrical resistivity

was measured by a dc 4 probe method between 10 and 300 K. The magnetic susceptibility was measured by a SQUID magnetometer between 5 and 300 K, and by a magnetic balance between 300 and 800 K. The magnitude of the induced magnetic field at the measurement by the SQUID magnetometer was 5000 Oe. The obtained magnetic susceptibility was corrected by subtracting the core diamagnetism of the relevant ions. The Seebeck coefficient was measured between 77 K and room temperature.

RESULTS AND DISCUSSION

A. Powder x-ray diffraction

Figure 1 shows the x-ray-diffraction patterns for $Sr_{2-x}La_xRhO_4$ ($x=0.0$, 0.5, and 1.0). It is obvious that a single phase was obtained for $Sr_{2-x}La_xRhO_4$ ($0.0 \leq x \leq 0.8$). Some unknown peaks were found in the patterns $x=0.9$, 0.95, and 1.0. The intensity of these peaks became large with an increase of x. Although tetragonal symmetry has been reported for $SrLaRhO_4$,[5] the symmetry of the crystal has been proved to be orthorhombic. The length of the axes are $a=0.5500$ (± 0.0001) nm, $b=0.5589$ (± 0.0001) nm, and $c=1.2537$ (± 0.0002) nm. Similar orthorhombic distortion has been found for Sr_2RhO_4 in our previous study,[4] $a=0.54518$ (± 0.00001) nm, $b=0.54487$ (± 0.00001) nm, and $c=1.2879$ (± 0.00001) nm, although it was known to be tetragonal.[3]

Figure 2 shows the composition dependence of the lattice-parameter and unit-cell volume. Since the slight orthorhombic distortion of Sr_2RhO_4 is considered to vanish in the compositions $x=0.1$, 0.3, 0.5, and 0.6 in Fig. 2, the length of the tetragonal a axis multiplied by $\sqrt{2}$ is indicated in order to compare with the length of orthorhombic a and b axes directly. It is clearly shown in Fig. 2 that the c axis (in a direction perpendicular to the RhO_2 plane) shortens as x increases, whereas the a and b axes

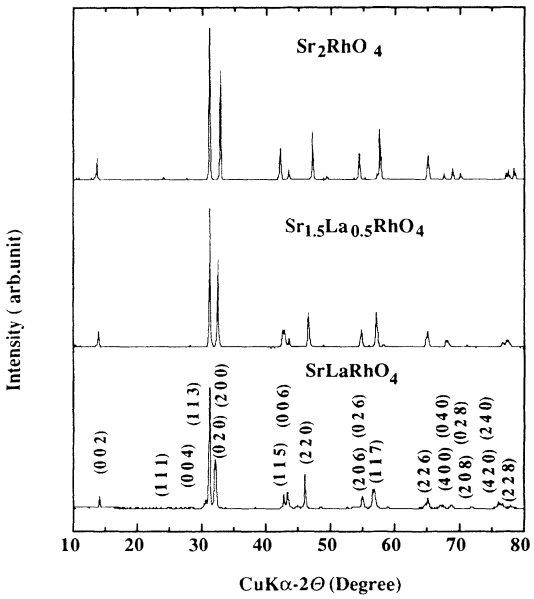

FIG. 1. Powder x-ray-diffraction patterns of $Sr_{2-x}La_xRhO_4$, $x=0.0$, 0.5, and 1.0.

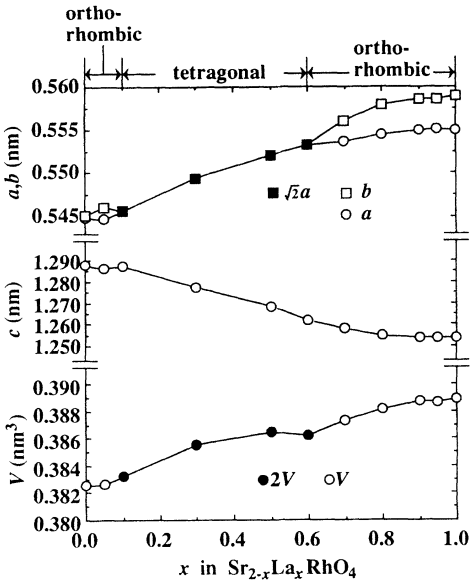

FIG. 2. Lattice parameters and unit-cell volume of $Sr_{2-x}La_xRhO_4$.

(in a direction parallel to the RhO_2 plane) on the contrary stretch. This result can be interpreted by considering the difference of the ionic radii between La^{3+} and Sr^{2+} and between Rh^{4+} and Rh^{3+}. In a K_2NiF_4-type structure, the change of the ionic radius of the A-site ion causes a drastic change in the length of the c axis, and the change of ionic radius of the B-site ion causes a drastic change in the length of the a and b axes.[8] The ionic radii of La^{3+} and Sr^{2+} at the nine coordination sites are 0.1216 and 0.131 nm, respectively, and the radii of Rh^{4+} and Rh^{3+} at the six coordination sites are 0.060 and 0.0665 nm,[9] respectively. Therefore the unit-cell volume should increase as x increases. The slight orthorhombic distortions for Sr_2RhO_4 and $Sr_{1.95}La_{0.05}RhO_4$ have been confirmed by the calculation of lattice parameters in making use of the structural analysis program by Izumi *et al.*[10] The possible space groups were *Fmmm* (No. 69) and *Bmab* (No. 64), and analysis based on the space group *Bmab* always gave the smaller R_{wp} factor for both Sr_2RhO_4 and $Sr_{1.95}La_{0.05}RhO_4$.

B. Resistivity

The resistivity versus temperature relation of $Sr_{2-x}La_xRhO_4$ for ($0.0 \leq x \leq 0.5$) and ($0.6 \leq x \leq 1.0$) are shown in Figs. 3 and 4, respectively. It is clearly shown by Fig. 3 and the inset figure in Fig. 3 that in the region $0.0 \leq x \leq 0.5$ the absolute value of the resistivity of each composition does not change regularly with x, and the profile of each temperature dependence is not monotonous but obviously changes with an increase of x. The positive temperature coefficient down to 10 K appears in the case of $x \leq 0.15$. In this metallic region the absolute value of the resistivity becomes small with an increase of x. The shape of the temperature dependence of resistivity for $x=0.0$ shows a marked difference from those for $0.05 \leq x \leq 0.15$. In the region $0.05 \leq x \leq 0.15$, the temperature coefficient of resistivity is always positive be-

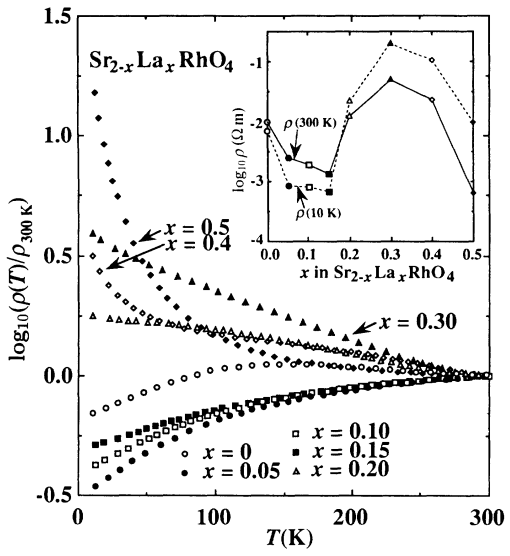

FIG. 3. Temperature dependence of the electric resistivity of $Sr_{2-x}La_xRhO_4$ ($0.0 \le x \le 0.5$) normalized with the value at 300 K. The positive temperature coefficient appears in the composition range $x \le 0.15$. Inset are the values of resistivities of $Sr_{2-x}La_xRhO_4$ ($0.0 \le x \le 0.5$) at 10 (dashed line) and 300 K (solid line).

tween 10 and 300 K, but Sr_2RhO_4 shows a broad maximum in resistivity between 100 and 200 K, and a negative temperature coefficient above 200 K.

In the case $x \ge 0.2$, the sign of the temperature coefficient of the resistivity from 300 to 10 K turns into negative in all samples, as shown in Figs. 3 and 4. In the region $0.2 \le x \le 0.5$, the absolute value of the negative temperature coefficient at 10 K becomes large with an increase of x. In the region $x \ge 0.6$, the resistivity of each composition increases with an increase of x, and the profile of each temperature dependence is similar. The largest value of resistivity at 300 K appears when $x = 0.95$. To investigate the details of temperature dependence of resistivity for semiconductive samples,

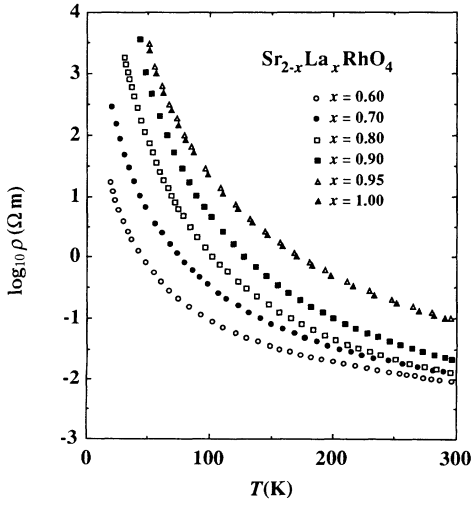

FIG. 4. Temperature dependence of electric resistivity of $Sr_{2-x}La_xRhO_4$ ($0.6 \le x \le 1.0$).

$e^{-1}\partial \log_{10}\rho(T)/\partial(k_BT)^{-1}$ was estimated from the experimental value of resistivity. Figures 5 and 6 show the $e^{-1}\partial \log_{10}\rho(T)/\partial(k_BT)^{-1}$ of $Sr_{2-x}La_xRhO_4$ ($0.2 \le x \le 0.5$) and $Sr_{2-x}La_xRhO_4$ ($0.6 \le x \le 1.0$) as a function of $\log_{10}T^{-1}$, respectively. If the conduction mechanism is one of the simple activation types, $e^{-1}\partial \log_{10}\rho(T)/\partial(k_BT)^{-1}$ should become independent of temperature and directly give the activation energy of the carrier. On the other hand, if the conduction mechanism is one of the variable range hopping[11] (VRH) types, the temperature dependence of the resistivity is expressed as

$$\rho(T) = \rho_0 \exp(T_0/T)^p ,$$
$$p = 1/(D+1) , \tag{1}$$

where D is the number of dimensions in conduction space. This type of conduction gives a linear relation $e^{-1}\partial \log_{10}\rho(T)/\partial(k_BT)^{-1}$ vs $\log_{10}T^{-1}$, thus the slope should give $-D/(D+1)$.[12]

As shown in Figs. 5 and 6, none of the samples shows a constant activation energy. The values of $e^{-1}\partial \log_{10}\rho(T)/\partial(k_BT)^{-1}$ for $Sr_{2-x}La_xRhO_4$ increase with an increase of temperature in the semiconductive region, except for $Sr_{1.5}La_{0.5}RhO_4$. The clearest linear dependence of $e^{-1}\partial \log_{10}\rho(T)/\partial(k_BT)^{-1}$ on $\log_{10}T^{-1}$ is observed for $Sr_{1.8}La_{0.2}RhO_4$ and $Sr_{1.7}La_{0.3}RhO_4$. In these samples, however, the slopes of $e^{-1}\partial \log_{10}\rho(T)/\partial(k_BT)^{-1}$ versus $\log_{10}T^{-1}$ are rather small compared to those expected from VRH. For $Sr_{1.8}La_{0.2}RhO_4$, the slopes above and below 40 K are -2.7 and -1.0, respectively, although this temperature region seems to be too narrow to evaluate exactly. For $Sr_{1.7}La_{0.3}RhO_4$, the slope between 20 and 200 K is -1.9. In the case of $Sr_{1.6}La_{0.4}RhO_4$, the slope between 40 and 120 K is about -0.6, and this value is close to the value -0.67, which is expected from the two-dimensional VRH conduction, but the coefficient below 40 K and above 125 K is almost equal to the value of

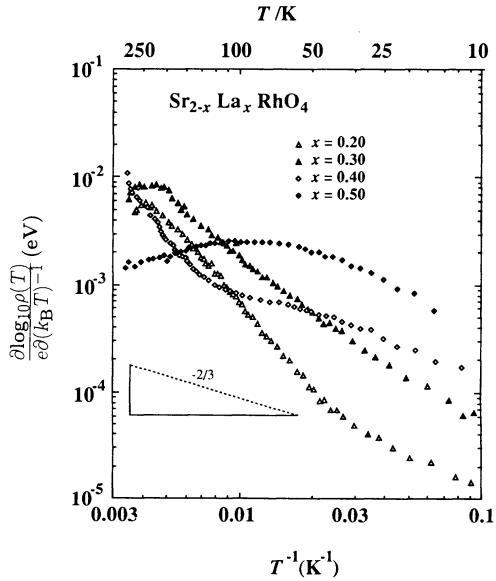

FIG. 5. Activation energy of carrier in $Sr_{2-x}La_xRhO_4$ ($0.2 \le x \le 0.5$) as a function of temperature.

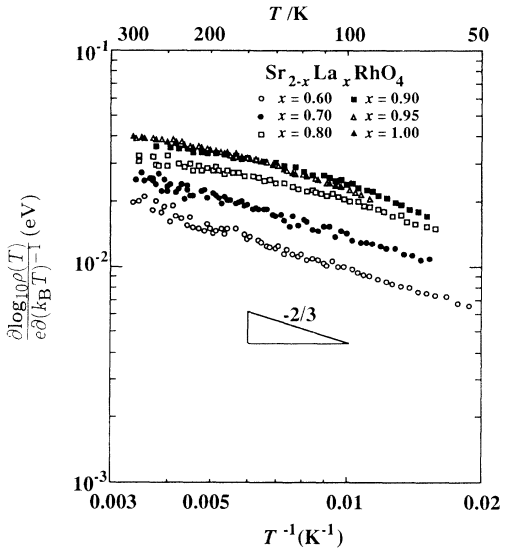

FIG. 6. Activation energy of carrier in $Sr_{2-x}La_xRhO_4$ ($0.6 \leq x \leq 1.0$) as a function of temperature.

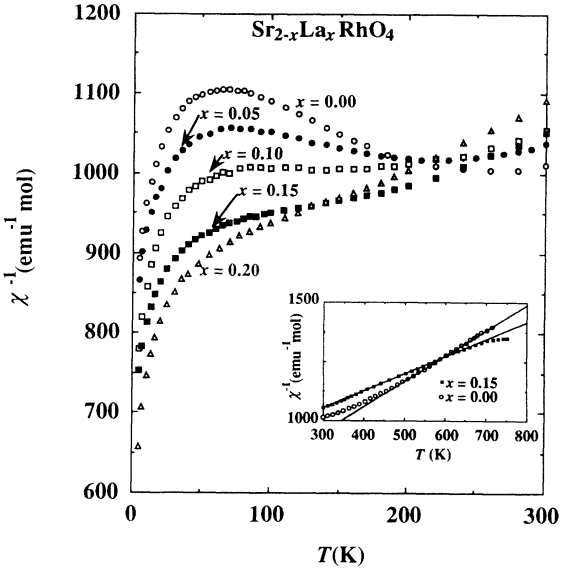

FIG. 7. Temperature dependence of χ_m^{-1} for $Sr_{2-x}La_xRhO_4$ ($0.0 \leq x \leq 0.2$) from 5 to 300 K. Inset are values of the χ_m^{-1} for Sr_2RhO_4 and $Sr_{1.85}La_{0.15}RhO_4$ above 300 K. The solid line represents the calculated values of χ_m^{-1} using the data shown in Fig. 10.

$Sr_{1.8}La_{0.2}RhO_4$ in these temperature regions. For $Sr_{1.5}La_{0.5}RhO_4$, a linear relation was not confirmed between $e^{-1}\partial \log_{10}\rho(T)/\partial(k_BT)^{-1}$ and $\log_{10}T^{-1}$. These results indicate that in the composition range $0.2 \leq x \leq 0.5$ there are plural types of conduction mechanisms, but neither are of the simple activation energy type nor the VRH type.

The value of $e^{-1}\partial \log_{10}\rho(T)/\partial(k_BT)^{-1}$ becomes somewhat greater in the low temperature region in the composition range $0.6 \leq x \leq 1.0$. It is clear that the absolute value of $e^{-1}\partial \log_{10}\rho(T)/\partial(k_BT)^{-1}$ increases with an increase of x, and shows simple temperature dependence. At least, the values of $e^{-1}\partial \log_{10}\rho(T)/\partial(k_BT)^{-1}$ for $Sr_{1.4}La_{0.6}RhO_4$, $Sr_{1.3}La_{0.7}RhO_4$, and $Sr_{1.2}La_{0.8}RhO_4$ show linear dependence on $\log_{10}T^{-1}$ above 50 K, and their slopes are nearly -0.67. This evidence suggests the presence of two-dimensional VRH-type conduction. For $Sr_{1.1}La_{0.9}RhO_4$, $Sr_{1.05}La_{0.95}RhO_4$, and $SrLaRhO_4$ the values of $e^{-1}\partial \log_{10}\rho(T)/\partial(k_BT)^{-1}$ are almost equal, as shown in Fig. 6. The values of $e^{-1}\partial \log_{10}\rho(T)/\partial(k_BT)^{-1}$ for them increase with an increase of temperature, but they do not exhibit clear linear dependence on $\log_{10}T^{-1}$.

In summary, it is shown that there are several kinds of conduction mechanisms in the semiconductive region of $Sr_{2-x}La_xRhO_4$, and one of them is attributable to the two-dimensional VRH.

C. Magnetic susceptibility

Figures 7, 8, and 9 show the temperature dependence of the reciprocal of the molar magnetic susceptibility χ_m^{-1} for the samples with $0.0 \leq x \leq 0.2$, $0.3 \leq x \leq 0.7$, and $0.8 \leq x \leq 1.0$, respectively, and the inset in Fig. 7 shows the reciprocal of the magnetic susceptibility of Sr_2RhO_4 and $Sr_{1.85}La_{0.15}RhO_4$ up to 750 K. It is clearly shown in Fig. 7 that χ_m^{-1} of Sr_2RhO_4 has its maximum and minimum below 300 K. $Sr_{1.95}La_{0.05}RhO_4$ and $Sr_{1.90}La_{0.10}RhO_4$ also have both maximum and minimum below 300 K, but the height of the peaks became smaller with an increase of x. The temperature corresponding to the maximum of χ_m^{-1} apparently decreases with an increase of x. The temperature giving the minimum is about 280 K for Sr_2RhO_4, and 220 K for $Sr_{1.95}La_{0.05}RhO_4$. On the contrary, the temperature giving the maximum value of χ_m^{-1} is independent of x. The temperature giving the maximum is about 60 K for both Sr_2RhO_4 and $Sr_{1.95}La_{0.05}RhO_4$. In the case $x \geq 0.15$, there is neither a maximum nor minimum in χ_m^{-1} between 5 and 300 K. χ_m^{-1} increases with temperature from 5 to

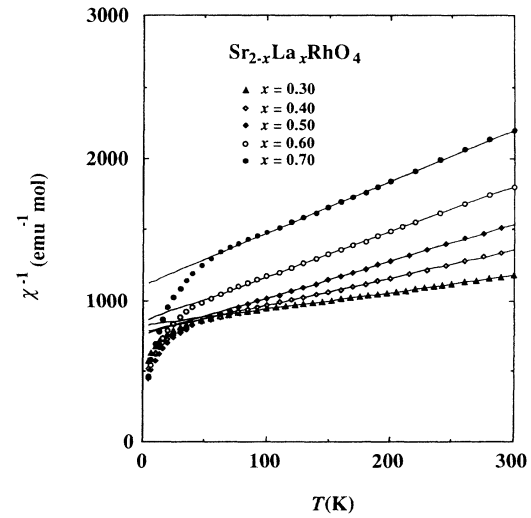

FIG. 8. Temperature dependence of χ_m^{-1} for $Sr_{2-x}La_xRhO_4$ ($0.3 \leq x \leq 0.7$) from 5 to 300 K. The solid lines represent the calculated values of χ_m^{-1} using the data shown in Fig. 10.

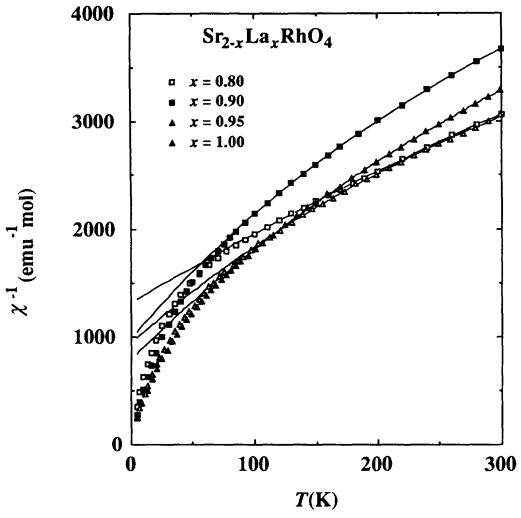

FIG. 9. Temperature dependence of χ_m^{-1} for $Sr_{2-x}La_xRhO_4$ ($0.8 \leq x \leq 1.0$) from 5 to 300 K.

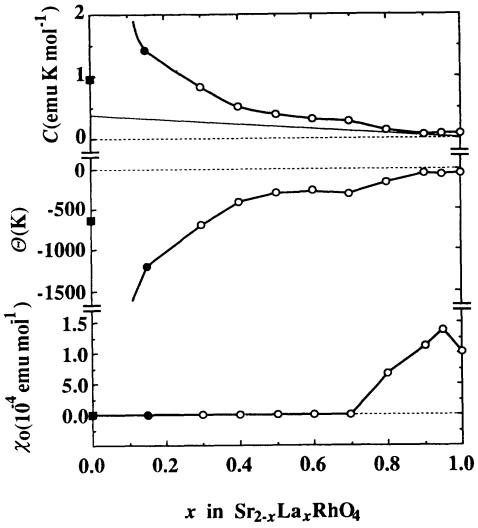

FIG. 10. Change in χ_0, C, and Θ with x for $Sr_{2-x}La_xRhO_4$. The temperature regions used for fitting are above 620 K for Sr_2RhO_4, from 400 to 600 K for $Sr_{1.85}La_{0.15}RhO_4$, and from 100 to 300 K for $Sr_{2-x}La_xRhO_4$ ($0.3 \leq x$). The solid line in C expresses the calculated C value supposing low-spin Rh^{4+} (and Rh^{3+}). The contribution of L is neglected in the calculation.

300 K, but there is still a small anomaly around 200 K, so it is impossible to fit χ_m^{-1} to the Curie-Weiss equation in certain temperature regions. Note that the temperature dependence of the resistivity in the metallic region ($x \leq 0.15$) is never simple Pauli paramagnetism. These facts suggest that the density of mobile charge carriers is fairly small compared to the density of localized charge carriers.

As shown by the inset figure in Fig. 7 the χ_m^{-1} values for Sr_2RhO_4 fall in a straight line above 620 K. The χ_m^{-1} values for $Sr_{1.85}La_{0.15}RhO_4$ also fall in a straight line between 400 and 600 K. Both values were fitted to the Curie-Weiss equation

$$\chi = C/(T-\Theta) , \tag{2}$$

where C is the Curie constant and Θ is the Weiss temperature. C and Θ values estimated through the least-squares fit of the experimental susceptibility to Eq. (2) are shown in Fig. 10, and the line in the inset in Fig. 7 expresses the χ_m^{-1} value calculated using these C and Θ data. Above 700 K the χ_m^{-1} values for $Sr_{1.85}La_{0.15}RhO_4$ become constant. It is certain that saturation of susceptibility is not due to the decomposition of samples from x-ray-diffraction analysis after the magnetic-susceptibility measurement. Thus this saturation of the χ_m^{-1} value is an intrinsic character of $Sr_{1.85}La_{0.15}RhO_4$.

In the case of $0.3 \leq x \leq 0.7$, it is clear that χ_m^{-1} values follow a linear relation on T, at least above 100 K, as shown in Fig. 8. Thus these samples exhibit Curie-Weiss-type paramagnetism above 100 K. The data of C and Θ estimated through the least-squares fit of magnetic susceptibility to Eq. (2) are shown in Fig. 10. The lines drawn in Fig. 8 express the calculated χ_m^{-1} values using the data of C and Θ shown in Fig. 10. In the case of $0.8 \leq x \leq 1.0$, a linear relationship does not hold between χ_m^{-1} and T, as shown in Fig. 9. In this case quite an excellent expression of magnetic susceptibility is given by the Curie-Weiss equation containing the temperature independent term χ_0:

$$\chi = C/(T-\Theta)+\chi_0 . \tag{3}$$

The data of C, Θ, and χ_0 estimated through the least-squares fit of the magnetic susceptibility to Eq. (3) are shown in Fig. 10, and the curves drawn in Fig. 9 express the calculated χ_m^{-1} values using the data shown in Fig. 10.

As shown in Fig. 10, the C value decreases with an increase of x in the region $x \geq 0.15$, and this tendency supports the low-spin state of Rh ions. The absolute value of C indicates the coexistence of a high-spin state of Rh ions along with low-spin Rh ions. In $SrLaRhO_4$, although there is a possibility of a small deficiency or an excess of oxygen, the formal valence of the Rh ion is thought to be nearly 3, but the C value 7.28×10^{-2} emu K/mol for $SrLaRhO_4$ is fairly great compared to 8.82×10^{-4} emu K/mol for $LaRhO_3$.[6] The experimental value of C is greater than the calculated C value supposing the mixing of low-spin Rh^{4+} and low-spin Rh^{3+} (solid line in Fig. 10), and the contribution of only the spin moment in the whole composition range.

The negative Θ indicates antiferromagnetic interaction between localized moments, and the absolute value of Θ becomes small as x increases in the region $0.15 \leq x$. This fact means that in this system there is antiferromagnetic interaction between localized moments, and the interaction becomes stronger with an increase of x. Thus this tendency of Θ indicates that antiferromagnetic order of moment occurs below about 200 K in the range $x \leq 0.2$.

The order of magnitude of χ_0 (10^{-4}–10^{-5} emu mol^{-1}) is comparable to the order of the temperature-independent Pauli paramagnetic term of mobile carriers. Thus the most reasonable origin of the χ_0 term is the Pauli paramagnetism of mobile carriers. But as shown in Fig. 4, the composition region where the χ_0 term grows

coincides with the region where resistivity becomes highest in this $Sr_{2-x}La_xRhO_4$ system, so it is not adequate to attribute the temperature-independent term to the paramagnetism of mobile carriers. Thus it is not proper to regard the grown χ_0 as the summation of Pauli paramagnetism and Landau diamagnetism of mobile carriers.

As a result, it seems that the apparent χ_0 term may originate from the localized moment. For example, in the case of $SrLaRhO_4$, Rh ions should take configurations of low-, intermediate-, or high-spin Rh^{3+}. Since the low-spin Rh^{3+} is a diamagnetic ion, positive experimental susceptibility must originate from intermediate- or high-spin Rh^{3+}. If the populations of intermediate- and high-spin Rh^{3+} are independent of temperature, and their magnetic interactions are negligibly small, the magnetic susceptibility should obey the simple Curie-type paramagnetism:

$$\chi_m = C/T \ . \tag{4}$$

As shown in Fig. 9, the experimental susceptibility is apparently different from the simple Curie type in Eq. (4). From the profile of the temperature dependence of susceptibility in Fig. 9, it seems that there is no magnetic ordering in $SrLaRhO_4$. Thus, the origin of the departure of experimental susceptibility from Eq. (4) may come from the increase of the magnitude of Rh^{3+} moment due to the thermal activation of Rh^{3+} ions from low-spin configurations to intermediate or high-spin configurations. For simplification, we suppose that the temperature dependence of susceptibility for $SrLaRhO_4$ is expressed as follows:

$$\chi_m = C(T)/T \ . \tag{5}$$

Here, $\chi_m T$ implies the Curie term as a function of the temperature. Figure 11 shows the $C(T)$ of $SrLaRhO_4$. Furthermore, assume that Rh^{3+} ions can take three different spin states, namely, low, intermediate, and high spin, and the energy difference between low-spin Rh^{3+} and intermediate-spin Rh^{3+} or between intermediate-spin Rh^{3+} and high-spin Rh^{3+} is equal to ε [see Fig. 11(b)]. Here, ε is contributed not only by the ligand field-splitting energy but also by the inner ion exchange energy (spin-flipping energy). Thus the expression giving the size of Rh^{3+} moments $S(T)$ and $C(T)$ becomes as shown below:

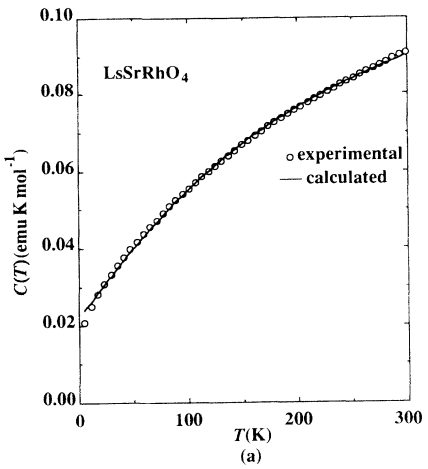

FIG. 11. (a) Temperature dependence of $C(T)$ for $SrLaRhO_4$ from 5 to 300 K. The solid line represents the calculated $C(T)$ using Eqs. (5) and (8). (b) Brief illustration of $4d$ electron configuration for Rh^{3+}.

$$S(T) = \frac{\exp(-\varepsilon/k_BT) + 2\exp(-2\varepsilon/k_BT)}{1 + \exp(-\varepsilon/k_BT) + \exp(-2\varepsilon/k_BT)} \ , \tag{6}$$

$$C(T) = \frac{N\mu_B^2}{3k_B} g^2 S(S+1)$$

$$\approx \frac{\exp(-\varepsilon/k_BT) + 2\exp(-2\varepsilon/k_BT) + 7\exp(-3\varepsilon/k_BT) + 6\exp(-4\varepsilon/k_BT)}{2\{1 + \exp(-\varepsilon/k_BT) + \exp(-2\varepsilon/k_BT)\}^2} \ . \tag{7}$$

In particular, the closest fit to the experimental data was achieved by introduction of the two parameters A and T_0 in Eq. (7):

$$C(T) \approx \frac{A\{\exp(-\varepsilon/k_BT') + 2\exp(-2\varepsilon/k_BT') + 7\exp(-3\varepsilon/k_BT') + 6\exp(-4\varepsilon/k_BT')\}}{2\{1 + \exp(-\varepsilon/k_BT') + \exp(-2\varepsilon/k_BT')\}^2} \ , \quad T' = T + T_0 \ . \tag{8}$$

The optimized values for ε, A, and T_0 are 0.0149(±0.0002) eV, 0.1431(±0.0008), and 113(±2) K, respectively. The calculated $C(T)$ from Eq. (8) is exhibited in Fig. 11(a) with a solid line. Here A is a factor adjusting the absolute value of $C(T)$. The presence of T_0 in Eq. (8) is considered to come from the fact that Boltzmann's activation factor $\exp(-\varepsilon/k_BT)$ becomes suddenly small as the parameter T approaches zero; how-

ever, the real parameter $T'=T+T_0$, which contributes directly to the spin flipping in Rh^{3+}, is the local lattice vibration mode, never ceasing even at $T=0$. The $C(T)$ curve fitting the experimental curve in Fig. 11(a) is fairly good except for the range $T \leq 20$ K. Based upon a two-state mode, e.g., the low-spin Rh^{3+} state ($S=0$) and the intermediate Rh^{3+} state ($S=1$), a similarly good fit to Fig. 11(a) could be obtained. Thus the behavior of magnetic susceptibility for $SrLaRhO_4$ can be explained by the thermal excitation of the Rh^{3+} ion. In the cases of $Sr_{2-x}La_xRhO_4$ ($x=0.8$, 0.9, and 0.95), the temperature dependence of the magnetic susceptibility is also explained via the thermal activation of the Rh ion from a low-spin state to an excited-spin state. But in these cases the existence of the Rh^{4+} ion disturbs the fit of susceptibility with Eq. (8), because when Rh^{4+} coexists with Rh^{3+} the number of adjustable parameters increases to six and there are several sets of suitable values of parameters.

Finally, the susceptibility is explained by the above mechanism from Eqs. (5) and (8), but the expression of susceptibility with Eq. (3) does not conflict with the experimental susceptibility, as shown in Fig. 9. It means that between 100 and 300 K expression (3) is the approximate form of the susceptibility.

D. Seebeck coefficient

Figure 12 shows the temperature dependence of the Seebeck coefficient (Q) of $Sr_{2-x}La_xRhO_4$. The positive sign for Q of all samples from 77 to 300 K suggests the hole conduction in this system. In the case $x \leq 0.5$, Q shows clear linear dependence on T. The equation giving the temperature dependence of the Seebeck coefficients of a highly degenerate electron gas predicts the linear dependence of Q on T:[13]

$$|Q| = 86.2(r+1)\frac{\pi^2}{3}(k_B T/E_F) , \tag{9}$$

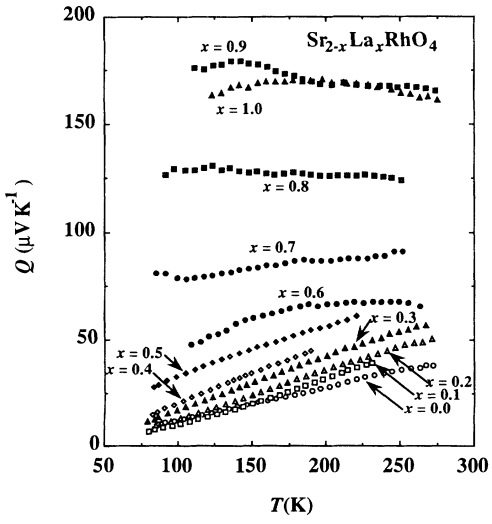

FIG. 12. Temperature dependence of Q for $Sr_{2-x}La_xRhO_4$ ($0.0 \leq x \leq 1.0$) from 77 to 300 K. The linear dependence of Q on T appears in the composition range $x \leq 0.5$.

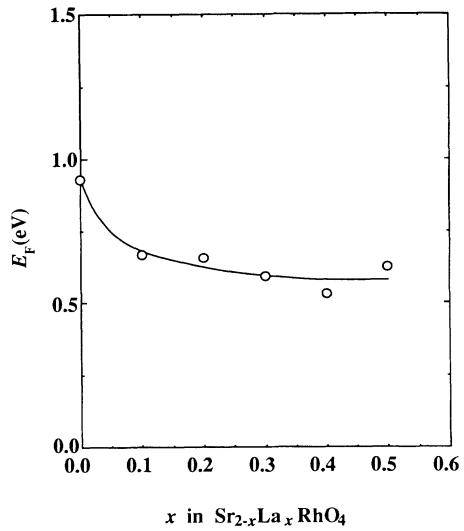

FIG. 13. Variation of Fermi energy vs x estimated from Q.

where the constant r is 1 for an ionic lattice, and E_F is the Fermi energy. Thus this experimental result indicates the existence of collective carriers, although the temperature dependence of the resistivity is not metallic, but is semiconductive when $x \geq 0.2$. Figure 13 shows the composition dependence of the Fermi energy estimated through the least-squares fit of experimental data of Q to Eq. (9). The decrease of E_F with x is clearly shown. This tendency may reflect the decrease of the number of mobile holes with La substitution.

The temperature dependence of Q of $Sr_{2-x}La_xRhO_4$ ($0.6 \leq x \leq 1.0$) is apparently different from that of $Sr_{2-x}La_xRhO_4$ ($0.0 \leq x \leq 0.6$). They do not exhibit linear dependence on T. Thus there are no collective carriers in the range $x \geq 0.6$.

Suppose that a Rh ion (Rh^{3+} or Rh^{4+}) takes a low-spin configuration, and all five or six $4d$ electrons occupy the $4d\varepsilon$ orbitals. In an oxide with K_2NiF_4-type structure, all three $d\varepsilon$ orbitals of the B ion have overlap to $p\pi$ orbitals of oxygen ions in the BO_2 plane. Thus in the case of low-spin Rh^{4+}, it is reasonable to assume that the hole in $4d\varepsilon$ orbitals becomes the carrier. The result of the Seebeck coefficient measurement supports this assumption.

CONCLUSION

From powder x-ray-diffraction analysis and Rietveld analysis for $Sr_{2-x}La_xRhO_4$ ($0 \leq x \leq 1$), orthorhombic distortion was recognized in the composition regions $0 \leq x \leq 0.05$ and $x \geq 0.7$. The positive temperature dependence of resistivity down to 10 K appears in the composition range $0.0 \leq x \leq 0.15$, and it turns to negative in the cases of $x \geq 0.2$. The temperature dependence of $e^{-1}\partial \log_{10}\rho(T)/\partial(k_B T)^{-1}$ suggests two-dimensional VRH conduction in the region $x \geq 0.6$. The shape of the temperature dependence of χ_m^{-1} remarkably changes at $x \geq 0.2$. The variation of Θ versus x suggests that the magnetic transition in the region $x \leq 0.2$ is an antiferromagnetic order of momentum. The estimated C values

are larger than the values expected from the contribution of only the spin term of low-spin Rh^{4+} and Rh^{3+} in all samples. The sign of the Seebeck coefficient is always positive, and the shape of the temperature dependence suggests the collective carrier in the region $x \leq 0.5$.

ACKNOWLEDGMENT

Part of this work was made possible by Grant-in-Aid for Scientific Research from the Ministry of Education, Science and Culture.

[1]D. Ganguli, J. Solid State Chem. **30**, 353 (1979).
[2]P. Poix, J. Solid State Chem. **31**, 95 (1980).
[3]J. J. Randhaul and R. Wold, J. Am. Chem. Soc. **81**, 2629 (1959).
[4]T. Shimura, M. Itoh, and T. Nakamura, J. Solid State Chem. **98**, 198 (1992).
[5]G. Blasse, J. Inorg. Chem. **27**, 2683 (1965).
[6]T. Nakamura, T. Shimura, M. Itoh, and Y. Takeda, J. Solid State Chem. **103**, 523 (1993).
[7]H. Levia, R. Kershaw, K. Dwight, and A. Wold, Mater. Res. Bull. **17**, 1539 (1982).
[8]B.-H. Chen and B. W. Eichhorn, J. Inorg. Chem. **97**, 340 (1992).
[9]R. D. Shannon, Acta Crystallogr. A **32**, 751 (1976).
[10]F. Izumi, H. Asano, H. Murata, and N. Watanabe, J. Appl. Crystallogr. **20**, 411 (1987).
[11]N. F. Mott, Adv. Phys. **21**, 785 (1975).
[12]B. Fisher, C. G. Kuper, G. Koren, S. Israelit, and L. Patlagan, Solid State Commun. **82**, 35 (1992).
[13]G. H. George, Jr. and M. J. Sienko, Inorg. Chem. **7**, 441 (1968).